ISSN 1063-7745, Crystallography Reports, 2020, Vol. 65, No. 7, pp. 1237–1241. © Pleiades Publishing, Inc., 2020.

SURFACE AND THIN FILMS

Optimization of EDTA–Ammonia Ratio for Chemically Deposited Layers of ZnO Nanoparticles

M. Önal[a],* and B. Altıokka[a],**

[a] *Bilecik Şeyh Edebali University, Bilecik, 11210 Turkey*

**e-mail: metehan.onal@bilecik.edu.tr*

***e-mail: baltiokka@gmail.com*

Received October 14, 2019; revised November 28, 2019; accepted December 3, 2019

Abstract—Layers of zinc oxide (ZnO) on glass substrates were grown by chemical bath deposition method. This method refers to solvo-thermal methods of crystal growth. When either ethylene-diamine-tetraacetic acid (EDTA) or ammonia was used as a complex agent, very weak adhesion of ZnO nanoparticles to the surface of glass substrates was noted, and when washing, the samples on the surfaces were removed by a water flow under pressure. When EDTA and ammonia were used together, the adhesion of ZnO nanoparticles to glass substrates increased dramatically. According to X-ray diffraction data, all sediments belong to the hexagonal syngony and correspond to the wurtzite-type ZnO structure. Optical absorption measurements showed that the band gap varied from 3.58 to 3.97 eV. The density of beams from ZnO nanowires on the substrate surface varied depending on the ratio between EDTA and ammonia.

DOI: 10.1134/S1063774520070135

INTRODUCTION

ZnO is an intriguing semiconducting material due to its band gap energy of 3.3 eV and exhibition of *n*-type feature [1]. Moreover, it has a large exciton binding energy (60 meV) and superior conducting properties based on oxygen vacancies in the wurtzite-type structure [2]. ZnO is considered as a potential material to be used in the fields of solid-state emission, piezoelectric transducers, solar cells, chemical sensors, ultraviolet laser diodes, photocatalysts, electroluminescent devices and transparent electrodes [1].

ZnO nanocrystalline structures can be produced by a variety of methods, such as ultrasonic spray pyrolysis, pulsed laser deposition, sol–gel methods and RF magnetron sputtering. In this work, ZnO nanoflowers were synthesized by the simple, safe and economic chemical bath deposition technique [3].

The issues of good adhesion and synthesis of homogeneous samples are a huge problem for this method because of the uncontrolled sample growth depending on unforeseeable chemical reactions. Therefore, a complex agent using an alkaline solution is preferred in many similar studies. Complex agents are generally chosen as monoethylamine, diethanolamine, ethylenediamine, ammonia, triethanolamine, dimethylamine, and their mixtures [4]. In the literature, in addition to ammonia, five complexing agents are used: N_2H_4 (hydrazine), ethylamine, methylamine, triethylamine, and dimethylamine [5].

There is only one study related to the agents prepared by mixing ethylene-diamine-tetraacetic acid (**EDTA**) and NH_3 for the chemically deposited ZnO [6]. However, the X-ray diffraction (**XRD**) patterns and optimum molarities of EDTA and NH_3 are not given. In addition, the samples were annealed for obtaining ZnO and quality of adhesion was not referred.

In this work, demonstrating a novel approach, certain amounts of EDTA and NH_3 were used together as a complexing agent to obtain good adhered samples. In contrast to the literature data, the samples were found to not adhere well when EDTA and NH_3 were used separately; and when the samples were rinsed with relatively pressurized water by using a washing bottle, they were completely removed from the glass substrate. On the contrary, when EDTA (8, 12 and 16 mM) and NH_3 were used in the final solution, the samples very tightly adhered to the glass substrates. Thus, the problem of poor adhesion was completely resolved in this study.

EXPERIMENTAL

Method

The chemical bath deposition was employed to produce layers of ZnO nanoparticles. The bath container and the glass substrates were cleaned with 10% HCl acid and then rinsed with deionized water. The temperature of the baths was kept at 85 ± 2°C and the depositions were completed in 20 min for all experi-

Table 1. The summarized experimental details for ZnO

Experiments	Concentration, mM		Temperature, °C	pH	Deposition time, min
	$ZnCl_2$	EDTA			
Set 1	65	4	85 ± 2	10.1	20
Set 2	65	8	85 ± 2	10.1	20
Set 3	65	12	85 ± 2	10.1	20
Set 4	65	16	85 ± 2	10.1	20
Set 5	65	20	85 ± 2	10.1	20

ments. When either EDTA or NH_3 was used, the samples adhered very poorly to the substrates and removed from the surface with water during the rinsing. In the 100 mL deionized water, firstly 65 mM $ZnCl_2$ was dissolved and then 4, 8, 12, 16 and 20 mM of EDTA were added; according to the EDTA–ammonia ratios, the experiments were named beginning from Set 1 to Set 5, respectively. In all the experiments, the pH of the solutions was adjusted 10.1 with diluted NH_3 and thereafter, the solutions started to be heated and stirred with 600 rpm. The summarized experimental conditions are listed in Table 1. When pH of the solutions was above or below 10.1, the precipitation was not observed on the surfaces. After the depositions, the samples were washed with water outgoing from the nozzle of the washing bottle and left to dry under room conditions.

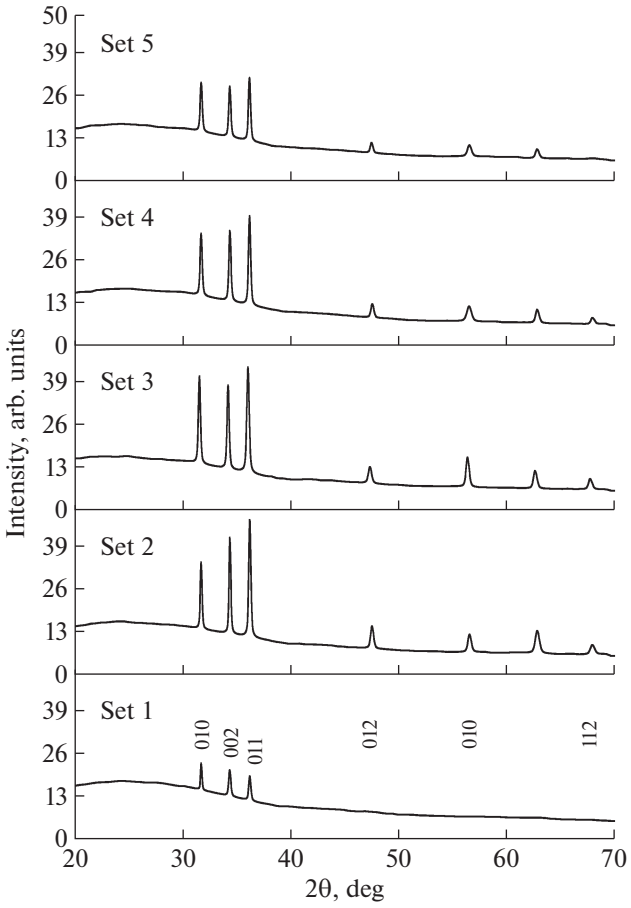

Fig. 1. Diffractograms of ZnO obtained using various EDTA–ammonia ratios.

Analysis

The structural, optical and morphological characteristic of the layers of ZnO nanoparticles were analyzed by using a PANalytical Empyrean XRD, JASCO V–530 with double beam UV-vis spectrometer and a Zeiss SUPRA 40VP scanning electron microscope, respectively.

RESULT AND DISCUSSION

Structural Analysis of Layers of ZnO Nanoparticles

The thicknesses of the layers of ZnO nanoparticles were calculated by using the well-known gravimetric method. The thicknesses of the layers obtained in Set 2 and Set 3 averaged 560 nm. The thickness of the layers of ZnO nanoparticles obtained in Set 4 was approximately 420 nm and the thicknesses obtained in Set 1 and Set 5 were on average 250 nm. These results showed that the adhesion of the layers of ZnO nanoparticles obtained in Sets 2–4 was relatively high and it depended on EDTA–NH_3 molarities. But the chemical reactions taking place in experiments could not be estimated for this outcome of good adhesion.

The structure of the layers of ZnO nanoparticles was studied by using XRD. Diffractograms are given in Fig. 1. All layers of ZnO nanoparticles are found to have hexagonal structures and to match well with ASTM card no 98-005-7450. The preferred orientation of the layers of ZnO nanoparticles was calculated by using the texture coefficient (*TC*) [7, 8]:

$$TC = \frac{I_{hkl}/I_{0hkl}}{\frac{1}{N}\sum_{N}\left(\frac{I_{hkl}}{I_{0hkl}}\right)}, \quad (1)$$

where I_{0hkl} is the standard intensity of the reflection from (*hkl*) plane given in ASTM card, I_{hkl} is the measured relative intensity of the *hkl* reflection. The calculated *TC* are given in Table 2. The preferred orientation of the layers of ZnO nanoparticles are found to be predominantly the (002) plane. However, from Table 2 it is clear that the method of chemical bath deposition of ZnO layers does not allow obtaining good ZnO textures on glass substrates. This phenomenon is also confirmed by the scanning electron microscopy (**SEM**) as will be discussed bellow.

The size of crystallites in the layers of ZnO nanoparticles was calculated via full width at half max-

imum (**FWHM**) of the peaks and using Scherrer equation:

$$cs = \frac{0.089 \times 180\lambda}{314\beta\cos\theta_C}\ [\text{nm}], \qquad (2)$$

where λ is the wavelength of X-ray radiation (1.54056 Å), β is the FWHM, $2\theta_C$ is the peak center [9–15]. The calculated crystallite sizes are summarized in Table 3. They vary between 29 and 48 nm. The thicknesses of layers of ZnO nanoparticles and EDTA–ammonia ratios are found to affect crystallite sizes.

Optical Properties of the Layers of ZnO Nanoparticles

The optical absorbance of the layers of ZnO nanoparticles was measured using the UV-vis spectrometer. The absorbance plots are given in Fig. 2. The layers of ZnO nanoparticles obtained in Set 1 and Set 5 showed relatively low absorbance. It was concluded that these results might be due to low thicknesses of layers of ZnO nanoparticles and low surface roughness.

Absorption coefficient (α) depends on the thickness of layers of ZnO nanoparticles (t) and also on band gap energy (E_g) according to Tauc plot model. This model was used in many studies [16–18]:

$$(\alpha h\nu)^2 = A(h\nu - E_g)^n, \qquad (3)$$

where $n = 1/2$ for directly allowed transitions, E_g is the optical band gap energy, $h\nu$ is the photon energy, and A is a constant. The direct band gap was estimated by extrapolating the linear portion of $(\alpha h\nu)^2$ to $h\nu = 0$ point [4, 11]. Tauc plots are given in Fig. 3 and estimated energy band gaps are listed in Table 3. The band gaps are between 3.58 and 3.97 eV, depending on the crystallite sizes. In the literature, the band gap of the ZnO is 3.3 eV [12, 13]. In our study, the band gap of layers of ZnO nanoparticles is greater than 3.3 eV. This may be due to small crystallite sizes.

Table 2. Calculated texture coefficients and preferred orientation of layers of ZnO nanoparticles

(*hkl*)	Set 1	Set 2	Set 3	Set 4	Set 5
(010)	1.18	0.79	1.05	0.92	0.98
(002)	1.29	1.45	1.26	1.32	1.29
(011)	0.53	0.75	0.69	0.76	0.73

Table 3. The crystallite sizes (*cs*) and energy band gaps of the layers of ZnO nanoparticles

Experiments	*cs*, nm				Band gap, eV
	(010)	(002)	(011)	Average	
Set 1	35	31	30	32	3.95
Set 2	46	47	30	41	3.67
Set 3	77	44	23	48	3.58
Set 4	33	36	32	37	3.80
Set 5	31	27	28	29	3.97

Fourier Transform Infrared Photometry of the Layers of ZnO Nanoparticles

The Fourier transform infrared photometer (FTIR) spectra were recorded between 380 and 4000 cm^{-1} (Fig. 4). The band positions and absorption peaks depend not only on the chemical composition

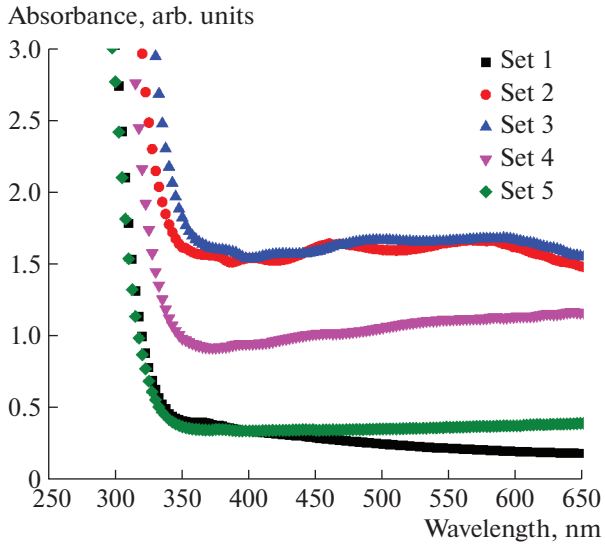

Fig. 2. Absorbance spectra of ZnO at wavelengths between 300 and 650 nm.

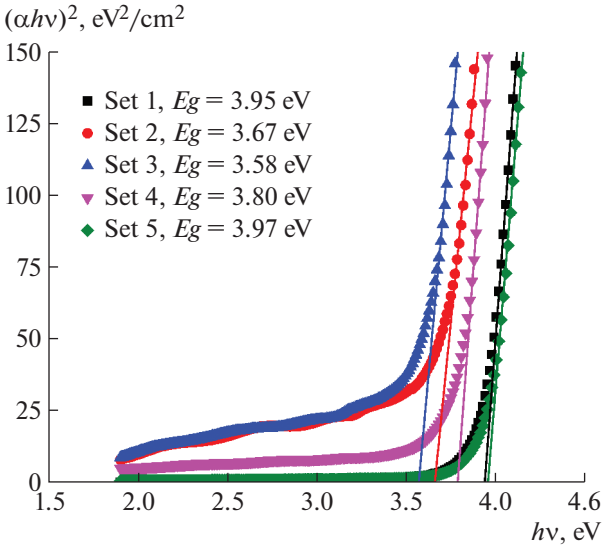

Fig. 3. Tauc plots and energy band gaps for layers of ZnO nanoparticles.

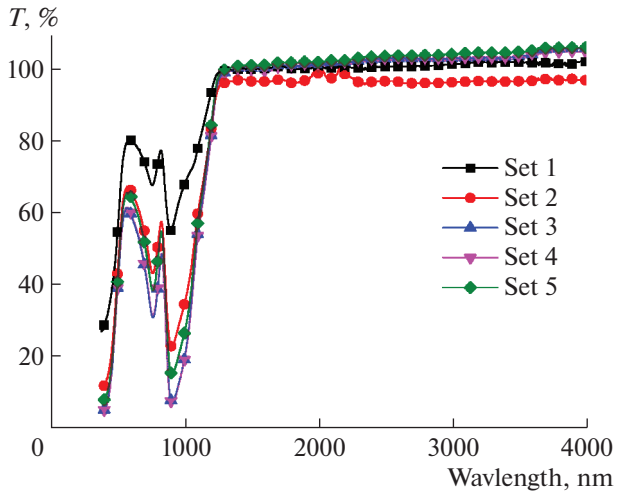

Fig. 4. FTIR spectra versus wavenumber for layers of ZnO nanoparticles.

and structure of the samples but also on the morphology of the samples [19]. Metal oxides generally show absorption bands in the fingerprint region below 1000 cm^{-1}, arising from interatomic vibrations [20]. In a previous study [21], ZnO stretching was observed at around 887 and 605 cm^{-1}. Thus, we can say that the vibrations near 725 and 900 cm^{-1} are related to ZnO.

SEM Analysis of the Layers of ZnO Nanoparticles

The 20 000 times magnified top view images of the layers of ZnO nanoparticles are given in Fig. 5. The nanorod-like structure of the surface of the samples obtained in Set 1 is observed (Fig 5a). The diameter and length of these sparse nanorods are approximately 150 and 750 nm, respectively. The surfaces of the samples obtained in Set 2 and Set 3 are covered completely with nanoflower-like structures (Figs. 5b and 5c). These flower-like structures decreased on the surface of the sample obtained in Set 4, as shown in Fig. 5d. The diameters of all flower-like structures are approximately 350 nm. There are almost no flowers or rod-like structures on the surface of the sample obtained in Set 5 (Fig. 5e). The possible reason for the relatively low absorbance of the samples obtained in Set 1 and Set 5 is a low surface roughness. Thus, these samples

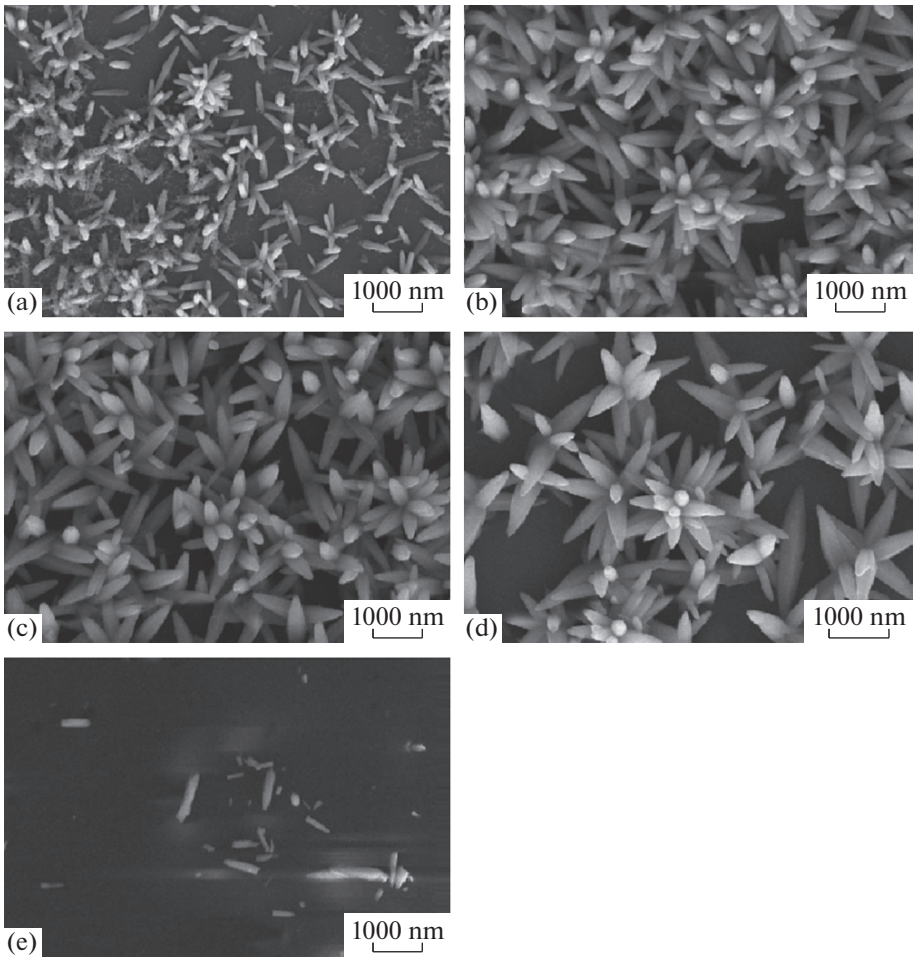

Fig. 5. 20 000 times magnified top view SEM images of the layers of ZnO nanoparticles obtained in (a) Set 1, (b) Set 2, (c) Set 3, (d) Set 4 and (e) Set 5.

Fig. 6. The photographs of the ZnO samples.

may be suitable for solar cells. On the contrary, the samples obtained in Sets 2–4 showed relatively high absorbance. So, these samples may be suitable for gas sensors because of the large surface area.

Visual Analysis of the Layers of ZnO Nanoparticles

Figure 6 shows the photos of all layers of ZnO nanoparticles. It can be seen that the ZnO nanoparticles adhere poorly to the surfaces of the samples obtained in Set 1 and Set 5. The other samples adhere well to the surface of the substrates. These sample surfaces turned out to be very compact. However, the reaction details for good adhesion cannot be analyzed.

CONCLUSIONS

In this study, layers of ZnO nanoparticles were grown by chemical bath deposition processes on the glass substrates. The great adhesion problem for chemically deposited ZnO was resolved by using certain amounts of EDTA and NH_3. When the concentration of EDTA was below 8 mM and above 16 mM, the samples did not adhere well to the surfaces of the glass substrates. The optimum conditions for good adhesion were when the concentration of $ZnCl_2$ was 65 mM, pH was 10.1 and the molarity of EDTA varied between 8 and 16 mM, as confirmed by photos of the samples. The structural analysis was carried out by XRD, all layers of ZnO nanoparticles had hexagonal crystal structures. While the band gap of bulk ZnO was 3.3 eV, the band gaps of the layers of ZnO nanoparticles were between 3.58 and 3.97 eV. The low crystallite sizes were concluded to be the reason for these high values of band gaps.

The SEM images showed that the surface of the samples was covered with nanoflowers. These nanoflowers are common morphologies of the ZnO particles produced by the chemical bath deposition. The density of the nanoflowers depended on the EDTA–ammonia ratio.

REFERENCES

1. M. M. Ali, J. Basrah Res. (Sciences) **37**, 49 (2011).
2. P. B. Taunk, R. Das, D. P. Bisen, et al., Karbala Int. J. Modern Sci. **1**, 159 (2015).
3. S. Temel, F. O. Gokmen, and E. Yaman, Eur. Sci. J., **13**, 28 (2017).
4. F. Özütok and S. Demiri, Digest J. Nanomater. Biostruct. **12**, 309 (2017).
5. H. Khallaf, G. Chai, O. Lupan, et al., J. Phys. D **42**, 135304 (2009).
6. Y. G. Taofeek and E. H. Olusegun, Int. J. Sci. Technol. Res. **1**, 24 (2012).
7. R. R. Krishnan, G. Sanjeev, R. Prabhu, and V. P. M. Pillai, JOM **70**, 739 (2018).
8. O. Reyes, D. Maldonado, J. Escorcia-García, and P. J. Sebastian, J. Mater. Sci.: Mater. Electron. **29**, 15535 (2018).
9. A. K. Yildirim, Materiali in Tehnologije **52**, 667 (2018).
10. A. S. Ibraheam, Y. Al-Douri, J. M. S. Al-Fhdawi, et al., Microsyst. Technol. **22**, 2893 (2016).
11. A. K. Yıldırım, Int. J. Eng. Res. Online **6**, 5 (2018).
12. R. Bhowmik, M. N. Murty, and E. S. Srinadhu, PMC Phys. B **1**, 20 (2008).
13. A. N. Fouda, M. Marzook, H. M. Abd El-Khalek, et al., Silicon **9**, 809 (2017).
14. S. I. Drapak, S. V. Gavrylyuk, Z. D. Kovalyuk, and O. S. Lytvyn, Inorg. Mater. **47**, 847 (2011).
15. L. N. Obolenskaya, M. A. Zaporozhets, G. M. Kuzmicheva, et al., Crystallogr. Rep. **60**, 406 (2015).
16. B. Thomas, S. Deepa, and K. Prasanna Kumari, Ionics **25**, 2 (2018).
17. K. L. P. Thi, L. T. Nguyen, N. H. Ke, et al., J. Electron. Mater. **47**, 6302 (2018).
18. Z. Yuan, J. Electron. Mater. **44**, 1187 (2015).
19. Z. R. Khan, M. S. Khan, M. Zulfequar, and M. Shahid Khan, Mater. Sci. Appl. **2**, 340 (2011).
20. H. Kumar and R. Rani, Int. Lett. Chem., Phys. Astron. **14**, 26 (2013).
21. M. R. Bodke, Y. Purushotham, and B. N. Dole, Cerâmica **64**, 91 (2018).

SPELL: OK